

THE CHUBUT GROUP (CRETACEOUS, GOLFO SAN JORGE BASIN): A SYNTHESIS OF ITS SEDIMENTARY PETROGRAPHY

Sabrina X. Olazábal^{1*}, Maisa A. Tunik^{2,3}, José M. Paredes¹, José O. Allard¹, Nicolás Foix^{1,2}

¹ Departamento de Geología (UNPSJB), Ciudad Universitaria S/N, Km4, Comodoro Rivadavia, Argentina.

² CONICET. Consejo Nacional de Investigaciones Científicas y Técnicas. Argentina.

³ Instituto de Investigación en Paleobiología y Geología (IIPG), Universidad Nacional de Río Negro-CONICET, General Roca, Río Negro, Argentina

*Corresponding author: sabrina.olazabal@unpata.edu.ar

ARTICLE INFO

Article history

Received March 9, 2025

Accepted June 4, 2025

Available online June 17, 2025

Handling Editor

M. Sol Raigemborn

Keywords

Detrital modes

Volcaniclastic input

Sediment routing

Provenance

Multiple source areas

ABSTRACT

This study presents a synthesis of petrographic analyses of the cretaceous Pozo D-129, Matasiete, Castillo, and Bajo Barreal formations in the Golfo San Jorge Basin, highlighting the influence of volcanic activity and sediment supply on the evolution of the Chubut Group. Data from outcrops in the San Bernardo Fold Belt and from the subsurface indicate that sandstone compositional variability was controlled by shifts in sediment source areas, linked to regional tectonic processes and active volcanism. Sandstones exhibit feldspatho-lithic and litho-feldspathic qFL, fQL, IQF to qLF composition detrital modes, with spatial and temporal variations in volcanic, pyroclastic lithic, feldspar and quartz components. The sediment sources for the outcrops in the San Bernardo Fold Belt include the Paleozoic igneous-metamorphic basement, Middle-Upper Jurassic volcanic and volcaniclastic rocks (Lonco Trapial Group), and acidic and pyroclastic sequences assigned to the Marifil Group. In contrast, the South Flank records a broader range of petrofacies, reflecting a combination of distal and local sources. In addition to the provenance of the Andes Cordillera, this sector received sediment contributions from Jurassic rocks exposed in the Deseado Region and older crystalline basement units. Andean volcanism dominates across all units, contributing direct volcanic ash fallout and reworked pyroclastic material.

INTRODUCTION

Reconstructing the tectonic and paleogeographic history of sedimentary basins relies heavily on sediment provenance studies, which provide critical insights into the origins and pathways of detrital components (Dickinson *et al.*, 1983). These analyses help identify sediment sources, tectonic settings, and transport processes, offering a clearer understanding of sediment-routing systems and their evolution over

time (Dickinson, 1985). Detrital modes, including sedimentary deposits' mineralogical and lithological composition, play a fundamental role in interpreting depositional environments and basin tectonic processes (Allen, 2017).

The Golfo San Jorge Basin (GSJB) is an endorheic basin of central Patagonia filled by continental deposits during the latest Jurassic and Cretaceous, covered by Cenozoic marine and continental rocks. The Chubut Group contains a thick stratigraphic

record (up to 6,000 m in the deepest depocenters), and it has a significant economic interest in the occurrence of hydrocarbons (Figari *et al.*, 2021). Understanding temporo-spatial variations in the provenance of these continental records is essential for reconstructing the tectonic processes that influenced sediment-routing systems and basin evolution.

Although previous research has identified contributions from the Patagonian Andes and local basement uplifts (Umazano *et al.*, 2009; Limarino and Giordano, 2016), the sedimentary pathways and specific detrital modes characterizing the Chubut Group deposits remain insufficiently understood. This study addresses these gaps by synthesizing current knowledge on the Chubut Group units' sedimentary petrography and detrital composition. Although aspects of diagenesis are briefly addressed, they are presented only as a complementary part of the analysis of the detrital components, which constitute the primary focus of this work. By combining petrographic analyses with a detailed review of detrital modes, this work seeks to reconstruct sedimentary pathways and refine interpretations of basin evolution. This synthesis relies both on our own data (Olazábal *et al.*, this work) and on a broad range of previously published studies, such as Tunik *et al.* (2006), Umazano *et al.* (2009), Comerio *et al.* (2014), Ibáñez *et al.* (2015), Tunik *et al.* (2015), Limarino and Giordano (2016), Olazábal *et al.* (2020), Méndez *et al.* (2022), and Olazábal *et al.* (2022).

The text is organized into three sections aligned with the main large-scale depositional systems: i) Pozo D-129 and Matasiete depositional system, ii) Castillo Formation, and iii) Bajo Barreal Formation. To date, no systematical provenance studies have been carried out in the uppermost units of the Chubut Group (Laguna Palacios-Colhué Huapi formations). Each section provides the geological background, the analysis of detrital modes, and the sediment-routing systems. This integrated approach offers a comprehensive understanding of the sedimentary processes shaping the Cretaceous deposits of the Chubut Group, enhancing insights into the dynamic evolution of the sedimentary basin.

GEOLOGICAL SETTING

The GSJB is an intracratonic, centripetal depression that originated during the Middle Jurassic (174–163 Ma) and preserves a sedimentary record

approximately 8,500 meters thick, spanning from the Jurassic to the late Cenozoic. It is bounded by the Cañadón Asfalto Basin, the North Patagonian Massif, the Deseado Region, the Patagonian Precordillera, and the Atlantic platform (Figari *et al.*, 2015) (Figs. 1a, b). The tectonic evolution of the basin was influenced by NW-trending Paleozoic-Jurassic faults, which generated a structural framework comprising both compressional and extensional features (Allard *et al.*, 2025).

The GSJB's basement consists of Paleozoic igneous and metamorphic rocks intruded by granitic and hypabyssal bodies, with local occurrences of the Patagonian batholith (Giacosa, 2020). Overlying the Paleozoic basement, the Mesozoic stratigraphy begins with volcanic and volcanioclastic rocks of the Marifil Formation and Lonco Trapial Group, followed by the Las Heras Group, which represents the late synrift phase and consists of deep and shallow lacustrine deposits. The Chubut Group, deposited during a sag phase, consists of continental deposits with a significant proportion of reworked volcanioclastic material (Paredes *et al.*, 2025). It includes six formations: Pozo D-129, Matasiete, Castillo, Bajo Barreal, Laguna Palacios, and Lago Colhué Huapi (Fig. 1c), and are exposed along the San Bernardo Fold Belt (SBFB) (Fig. 1d). Typical exposures along the SBFB are shown in figure 2.

The Pozo D-129 Formation, the basal unit of the Chubut Group, extends over approximately 150,000 km² and reaches a maximum thickness of 1,500 m. It consists mainly of organic-rich black shales, which constitute the primary source rocks of the petroleum system (Figari *et al.*, 2021). These shales were deposited in perennial, meromictic lakes, as evidenced by laminated claystones, pyrite, and the lack of bioturbation, indicative of anoxic deep-water conditions (Basile *et al.*, 2014). This lacustrine system persisted for over 10 million years during the Barremian-Aptian, establishing the regional base level for coeval drainage systems originating from the basin margins (Paredes *et al.*, 2021).

The Matasiete Formation, partially coeval with the Pozo D-129 Formation, consists of fluvial channel-belt deposits interbedded with reddish floodplain deposits. According to Lesta *et al.* (1980), it is subdivided into three members (Lower, Middle, and Upper). The overlying Castillo Formation, up to 2,000 m thick, is composed of volcanioclastic deposits intercalated with fluvial channel belts and has been

dated by the U/Pb method and assigned to the Late Albian-Cenomanian (Allard *et al.*, 2022). The Bajo Barreal Formation, the primary hydrocarbon-bearing unit of the GSJB, currently accounts for approximately 32 % of the country's liquid hydrocarbon production.

This formation consists of fluvial deposits mainly composed of reworked pyroclastic material and is divided into Lower and Upper members (Sciutto, 1981). Fossil evidence from this unit constrains its age to the Cenomanian-Turonian (Casal *et al.*, 2021).

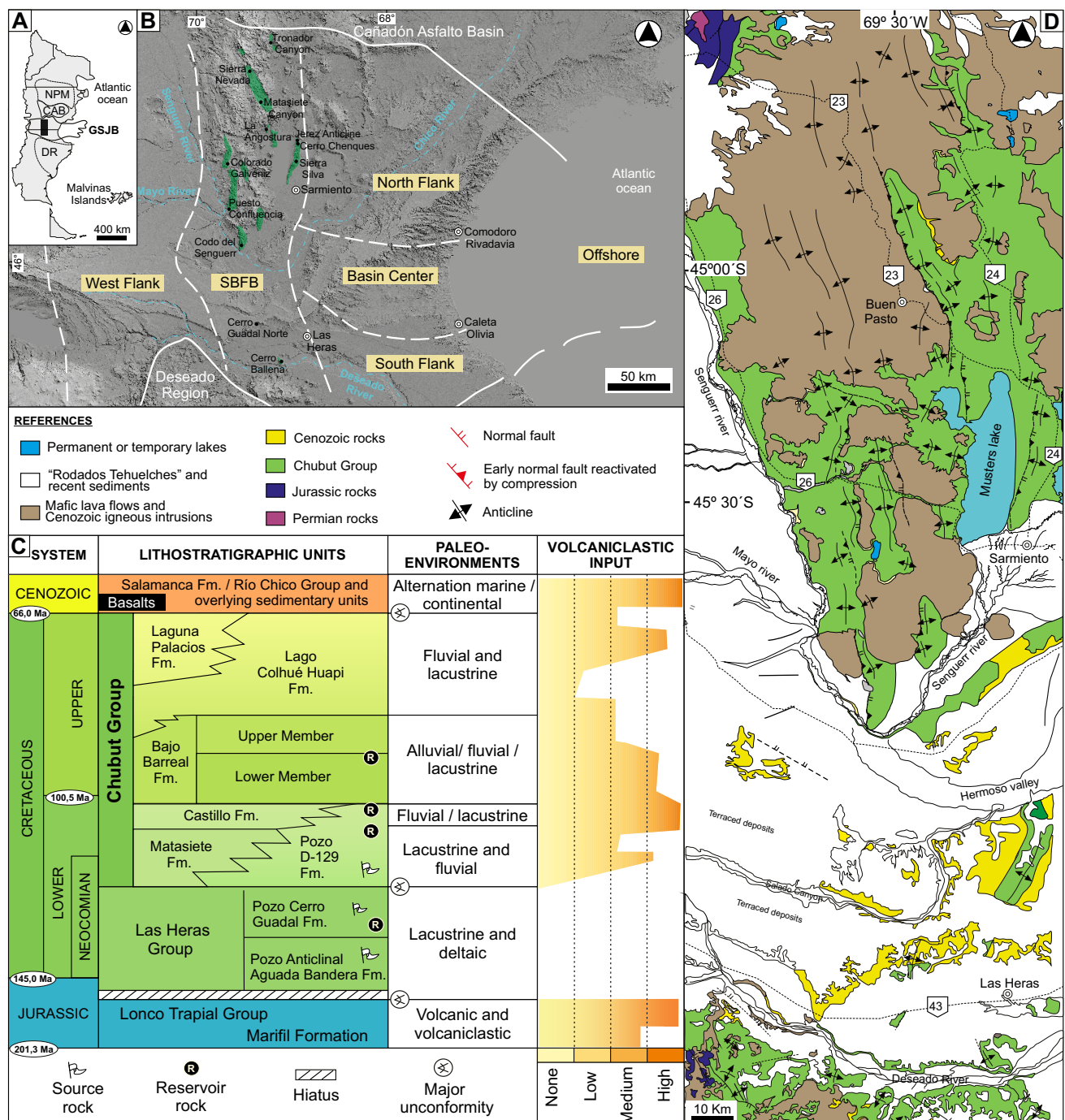


Figure 1. a) Location map of the GSJB within the extra-Andean Patagonia. Key: NPM= Nordpatagonian Massif; CAB= Cañadón Asfalto Basin; GSJB= Golfo San Jorge Basin; DR= Deseado Region. **b)** Structural framework of the Golfo San Jorge Basin, highlighting the San Bernardo Fold Belt (SBFB). The locations of all study localities analyzed in this work are shown. **c)** Stratigraphy of the GSJB (after Allard *et al.*, 2022). Notice the significant volcaniclastic input in the Chubut Group, a lithological feature that allows its differentiation from the underlying Las Heras Group. **d)** Simplified geological map of the SBFB, showing the major lithostratigraphic units and main tectonic structures.

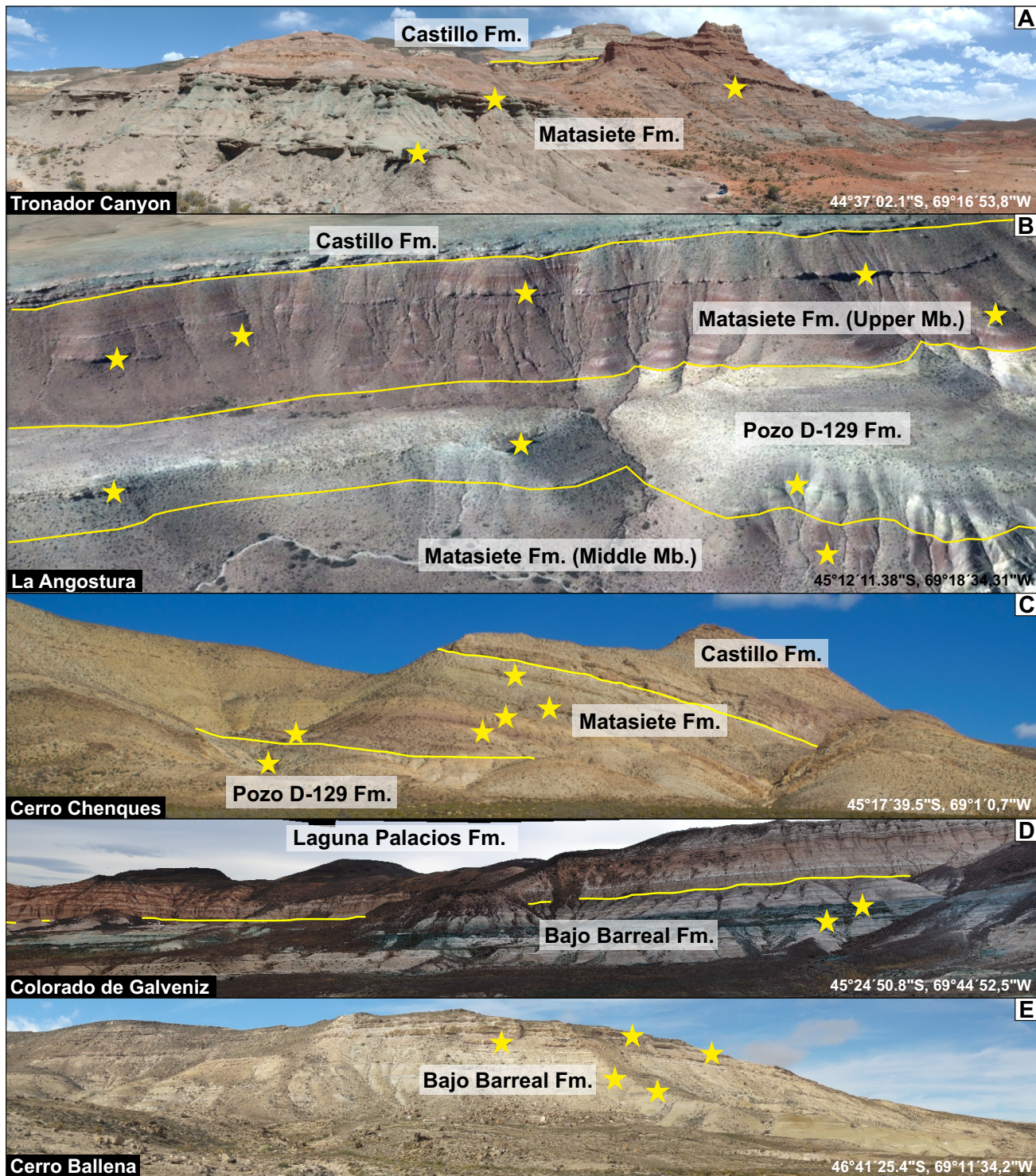


Figure 2. Exposures of the Chubut Group along the San Bernardo Fold Belt (SBFB). The images illustrate the stratigraphic relationships between the Pozo D-129, Matasiete, Castillo, Bajo Barreal, and Laguna Palacios formations, highlighting key lithological features. **a)** Tronador Canyon. **b)** La Angostura, illustrating the relationship between the Upper and Middle members of the Matasiete Formation, with intercalations of the Pozo D-129 Formation. **c)** Cerro Chenques in Sierra Silva. **d)** Colorado de Galveniz. **e)** Cerro Ballena anticline. The yellow stars indicate the location of samples collected for petrographic analysis and yellow lines indicate the formations limits.

The Lago Colhué Huapi Formation represents meandering fluvial systems and has yielded vertebrate fossils, including dinosaurs, with an age range spanning the Coniacian-Maastrichtian (Casal *et al.*, 2015). The overlying Laguna Palacios Formation, reaching up to 300 m in thickness, is composed of fluvial and eolian deposits containing abundant paleosols and ash-fall layers, indicating the presence of grassy vegetation and localized volcanic activity. The Cenozoic deposits in the GSJB record several transgressive-regressive second-order cycles (Foix *et al.*, 2025). The Salamanca Formation, which marks the first transgressive event during the late Maastrichtian, is followed by continental deposits associated with the middle Paleocene-middle Eocene Río Chico Group and the middle Eocene-lower Miocene Sarmiento Formation (Fig. 1d).

DETRITAL FINGERPRINTS

The Pozo D-129 - Matasiete Depositional System

During the deposition of this depositional system, the Cañadón Asfalto Basin was connected with the Golfo San Jorge Basin through two tectonic sedimentary corridors (Allard *et al.*, 2015). Petrographic analyses from multiple outcrops along a north-south transect prove this linkage, revealing distinctive compositional trends. These trends are expressed in the relative abundances of granular framework and are interpreted as reflecting variations in the lithologic composition of the source areas. The petrographic data (Figs. 3a, b) support a progressive change in provenance along the transect, discussed in the following section of the manuscript.

Sandstones of the Matasiete Formation, according to the proposal of Garzanti (2019), are feldspatho-lithic and qFL (Fig. 3b), with modal compositions ranging from Q6F30L64 for the Lower Member, Q8F31L61 for the Middle Member, and Q10F26L64 for the Upper Member (Table 1). Paleovolcanic lithic fragments with lathwork and microlitic textures (Fig. 4a) dominate these sandstones, followed by felsitic, glassy, and devitrified textures. Igneous-metamorphic and sedimentary lithic fragments occur in minor proportions, while feldspar grains consist mainly of alkali feldspars. Quartz is present as monocrystalline and polycrystalline grains. Accessory minerals include biotite, undifferentiated opaques, and distinctive euhedral pyroxenes, and

amphiboles, the latter showing twinning and opaque rims (Fig. 4b). Notably, the abundance of heavy minerals, particularly pyroxenes and amphiboles, decrease progressively from Tronador Canyon to Matasiete Canyon (Figs. 1b, 2a).

The Lower, Middle, and Upper members of the Matasiete Formation exhibit a decrease in basic-intermediate lithic fragments, which becomes more pronounced in the Pozo D-129 Formation, where pyroclastic lithic fragments increase significantly. This shift is reflected in modal compositions, with the Pozo D-129 Formation south of La Angostura (Fig. 2b) reaching Q20F44L36 (Table 1) and are classified as IQF, qLF, and qFL (Figs. 3a, 4c). The southern exposures of Pozo D-129 Formation are represented by samples from the Codo del Senguerr, which are feldspatho-lithic, qFL and fQL (Fig. 3a).

In the Pozo D-129 Formation, facies variability is evident, particularly in the Cerro Chenques of the Sierra Silva anticline (Fig. 2c), where the formation reaches ~43 m in thickness and is divided into lower, middle, and upper informal sections (Paredes *et al.*, 2014). The lower section comprises oolitic grainstones (Fig. 4d) containing silicified ooids with concentric laminar microstructures, often characterized by neovolcanic pumice nuclei (Olazábal *et al.*, 2021). The middle section exhibits a mixed siliciclastic-carbonate-pyroclastic composition, with significant proportions of quartz, feldspar, paleovolcanic, and neovolcanic lithic fragments, along with ooids and bioclasts (Fig. 4e). The upper section lacks carbonate components, with up to 30 % of pyroclastic fragments.

Oolitic grainstones of the Pozo D-129 Formation exposed at the Jerez Anticline, located 1,5 kilometers northward of the Cerro Chenques, exhibit a grain-supported microfabric, with the ooids displaying a broader range of internal microstructures. These include concentric laminar patterns, irregularly edged forms—also called cerebroid—and, in some cases, spiny, deformed, or composite structures. Additionally, these ooids commonly contain a variety of nuclei, such as neovolcanic shards. Unlike the Cerro Chenques succession, the greater diversity of ooid morphotypes suggests deposition under variable bathymetric conditions, including littoral environments influenced by wave action, vadose zone, and affected by subaerial exposure. Their coexistence within these deposits indicates reworking and sedimentation in a very shallow water environment, distinguishing them

Table 1		Section	Locality	Qm	Qp	Qrv	Fk	Pl	Lbi	Lac	Lpy	Lpm	Lse	Lal	Cze	CCa	CAr	Cfe	Po	Mx	Ot	Op	Hc	Total
Castillo Fm.	La Angostura (n=7)	Tronador Canyon	2,2	0,0	0,2	15,6	8,9	16,9	5,8	16,0	0,0	4,4	4,9	18,2	3,3	0,0	0,0	0,7	2,4	0,2	0,2	0,0	100,0	
			3,6	0,0	0,7	22,4	13,8	10,7	7,1	15,1	0,4	0,0	2,9	4,9	3,6	10,0	0,9	3,3	0,0	0,0	0,7	0,0	100,0	
			3,3	0,2	0,4	15,1	6,9	8,0	2,7	33,6	0,2	0,0	2,9	4,4	0,0	0,0	0,0	0,5,1	16,7	0,0	0,4	0,0	100,0	
			6,7	0,0	0,9	13,6	16,0	7,1	3,3	41,6	0,0	0,2	4,7	0,0	1,6	0,7	0,2	3,3	0,0	0,0	0,2	0,0	100,0	
			8,0	0,0	0,0	15,6	17,8	11,8	3,3	26,2	1,1	0,0	2,7	0,0	1,1	9,6	0,0	2,9	0,0	0,0	0,0	0,0	100,0	
			2,9	0,0	0,0	18,0	7,3	5,6	6,2	56,4	0,0	0,0	1,8	0,0	0,0	0,0	0,0	1,1	0,0	0,7	0,0	0,0	100,0	
			10,4	0,0	0,2	19,2	12,0	5,6	8,6	25,4	0,0	0,0	2,0	0,0	0,0	6,8	1,0	2,2	6,6	0,0	0,0	0,0	0,0	100,0
	Sierra Nevada (n=10)	7,4	0,2	0,6	11,0	3,6	15,6	9,0	13,8	1,8	0,0	7,0	0,2	16,6	0,2	0,0	9,8	0,0	2,2	1,0	0,0	100,0		
		8,2	0	0,6	6,6	3,8	3,8	8,4	15,4	0,0	0,0	7,0	4,2	0,0	1,2	1,0	23,6	8,8	2,4	4,8	0,0	99,8		
		5,6	0,2	0,6	12,0	7,6	12,4	12,2	1,8	2,0	0,4	5,4	5,6	8,0	0,0	0,2	22,0	0,0	3,2	0,8	0,0	100,0		
Upper Mb. Matasiete Fm.	Matasiete Canyon (n=8)	7,6	0,2	0,8	9,6	3,6	3,0	4,2	8,6	0,6	0,0	2,2	9,8	0,0	7,8	0,6	20,8	0,0	9,2	11,4	0,0	100,0		
		3,6	0	1,8	13,6	5,2	5,8	6,2	3,6	1,2	0,4	7,4	0,2	21,0	3,6	0,2	7,4	0,0	16,6	2,2	0,0	100,0		
		4	0,2	0	7,6	5,6	22,8	11,4	7,2	1,6	0,2	3,4	8,8	7,2	1,2	0,2	16,0	0,0	2,4	0,2	0,0	100,0		
		7,8	0,4	0	10,0	5,8	7,6	17,6	10,6	1,4	0,4	1,6	6,2	0,0	12,0	1,4	13,6	0,0	2,0	1,6	0,0	100,0		
		5,2	0,6	0	9,0	4,4	7,2	16,8	7,8	0,8	0,4	4,4	18,0	0,2	2,6	0,4	18,6	0,0	2,0	1,4	0,0	99,8		
		4,8	0,6	0,4	6,4	3,0	13,8	19,4	14,0	2,2	0,4	3,0	8,6	0,0	1,6	0,2	20,6	0,0	0,8	0,2	0,0	100,0		
		4	1	0,2	6,6	3,6	5,4	7,8	25,2	0,4	0,2	4,2	17,4	0,0	3,2	1,2	16,8	0,0	1,8	1,0	0,0	100,0		
	Matasiete Canyon (n=6)	2,8	0,4	0,4	8,2	4,0	11,4	11,0	14,2	1,4	0,2	3,8	12,8	16,6	0,4	0,6	9,8	0,0	1,8	0,2	0,0	100,0		
		2,8	0	0,8	8,6	6,4	6,4	32,4	0,2	0,0	2,2	5,0	10,6	0,6	3,2	10,2	0,0	2,0	0,4	0,0	99,8			
		3,6	0,6	0,2	11,8	5,2	13,2	4,2	25,8	1,6	0,0	4,0	12,8	0,0	0,2	0,0	8,2	0,0	5,2	3,4	0,0	100,0		
Middle Mb. Matasiete Fm.	Matasiete Canyon (n=14)	4	0,2	0,8	10,0	2,4	8,2	3,8	21,2	0,6	0,2	4,6	17,8	0,0	0,2	0,0	16,6	0,0	6,6	2,6	0,0	99,8		
		3,4	0,2	0,4	13,6	7,0	14,0	7,2	7,0	3,8	0,2	4,0	17,2	0,0	1,2	0,0	17,6	0,0	2,2	1,0	0,0	100,0		
		3,6	0,6	0	9,8	5,8	18,4	6,6	7,2	1,8	0,2	6,2	0,0	18,8	0,0	0,0	16,6	0,0	3,6	0,8	0,0	100,0		
		6,2	0,2	0,0	10,6	9,2	7,6	7,4	8,6	1,2	0,0	5,4	8,4	0,8	17,8	3,0	9,8	0,0	0,4	3,4	0,0	100,0		
		3,5	0,2	0,6	8,1	11,4	11,6	9,3	5,8	1,0	0,0	5,6	8,1	0,2	15,1	6,2	8,1	0,0	0,2	5,2	0,0	100,0		
		1,6	0,8	0,8	6,6	6,4	6,8	4,4	29,4	0,2	0,0	5,6	24,8	0,0	3,6	0,6	8,2	0,0	0,0	0,2	0,0	100,0		
		5,5	0,2	0,0	3,8	4,4	9,8	9,3	16,4	0,0	0,0	2,9	14,4	0,0	18,4	0,2	14,2	0,0	0,0	0,2	0,0	99,9		
	Pozo D-129 Fm.	3,2	0,0	0,4	7,6	5,8	6,6	5,4	2,6	2,2	0,0	5,6	19,6	1,0	18,4	2,8	14,6	0,0	0,2	4,0	0,0	100,0		
		7,2	0,4	0,2	4,0	5,0	4,6	5,4	7,8	2,2	0,0	0,0	7,8	0,0	7,8	0,0	46,4	0,0	0,0	1,2	0,0	100,0		
		5,8	0,2	0,2	6,8	10,0	11,0	7,2	6,0	1,2	0,0	3,2	21,6	1,8	2,8	0,8	20,8	0,0	0,0	0,6	0,0	100,0		
Pozo D-129 Fm.	Codo del Senguer (n=9)	2,0	0,0	0,8	5,0	12,6	15,2	7,8	9,0	1,0	0,0	4,2	0,0	40,2	0,0	0,0	2,2	0,0	0,0	0,0	0,0	100,0		
		3,0	0,2	0,2	10,4	4	8	8	29,8	0,0	0,0	4,0	13,6	0,0	5,0	0,0	13,8	0,0	0,0	0,0	0,0	100,0		
		7,0	0,4	0,2	14,8	6,6	7,2	9,8	13,8	0,8	0,0	4,4	9,6	8,2	4,8	0,0	9,6	0,0	0,0	2,8	0,0	100,0		
		5,0	0,6	0,4	17,4	6,8	19	9	9,4	0,2	0,0	4,4	0,0	8,6	2,4	0,0	13,8	0,0	0,0	3,0	0,0	100,0		
		5,8	0,4	0,4	13	6	11,8	2,8	5,4	0,4	0,0	5,4	26,2	1,4	5,0	1,4	5,6	0,0	0,6	8,4	0,0	100,0		
		3,0	0,8	0,2	10,8	6,6	10,2	8,6	8,4	0,0	0,0	7,6	26,0	0,2	4,4	2,2	6,2	0,0	0,8	4,0	0,0	100,0		
		2,4	0,8	0,0	11,6	3,6	15,6	4,4	10,6	0,2	0,0	5,6	8,0	11,0	1,4	1,4	19,0	0,0	0,0	4,4	0,0	100,0		
	Lower Mb. Matasiete Fm.	2,8	0,0	0,2	19,4	5	11,2	7	16,8	0,4	0,0	3,8	1,4	2,4	2,0	1,4	5,4	0,0	0,2	2,6	0,0	100,0		
		3,4	0,0	0,2	16,2	3	13,8	8,6	5,4	0	0,0	7,6	0,0	6,8	23,2	0,6	5,0	0,0	0,0	6,2	0,0	100,0		
Lower Mb. Matasiete Fm.	Matasiete Canyon (n=14)	2,4	0,2	0,0	10,8	5	24,6	12,4	4,2	0,6	0,0	6,0	6,8	17,8	0,6	2,6	5,2	0,0	0,0	0,8	0,0	100,0		
		2,0	0,4	0,4	17,6	5,4	15,4	4,8	4	0,2	0,2	6,8	7,6	14,8	6,0	2,0	7,2	0,0	0,2	5,0	0,0	100,0		
		3,0	0,0	0,0	19,4	4,8	18,2	8	5,4	0,2	0,0	5,0	1,8	3,4	21,2	1,8	4,8	0,0	0,2	2,8	0,0	100,0		
		3,2	1,0	0,2	12,2	6	17,2	19	2,4	0,4	0,0	12,2	0,0	0,4	23,8	0,4	1,2	0,0	0,0	0,4	0,0	100,0		
		4,6	0,8	0,6	13,2	7,2	13,2	18,4	1,8	0,6	0,0	5,8	6,8	16,0	4,0	3,8	0,0	0,0	1,4	0,0	100,0			
		2,2	0,2	0,2	11,4	4,6	12,6	12,4	13,4	0,8	0,2	7,6	2,8	0,0	16,0	0,2	12,8	0,0	0,2	2,4	0,0	100,0		
		3,8	0,4	0,8	14,4	7,8	10,6	18	0,2	0,6	0,8	9,4	0,0	0,2	20,8	2,8	6,4	0,0	0,6	2,4	0,0	100,0		
	Codo del Senguer (n=9)	3,4	0,4	0,4	14,8	4	21,8	12,4	6	0,4	0,2	5,8	0,0	18,8	9,2	0,0	2,0	0,0	0,0	0,4	0,0	100,0		
		1,6	0,4	0,8	13	5	17,8	5	1,8	0,2	0,4	8,2	17,8	5,4	8,2	0,0	2,0	0,0	0,2	2,2	0,0	100,0		
		4,0	0,0	0,6	11,4	7,8	18,4	17,4	1,4	0,4	0,2	7,2	8,8	0,0	10,2	3,0	3,8	0,0	0,8	4,6	0,0	100,0		
Pozo D-129 Fm.	Codo del Senguer (n=9)	5,0	0,2	0,4	16	7,2	14,6	16,6	1	0,0	0,0	6,4	2,2	0,2	18,2	1,8	2,6	5,6	0,6	1,4	0,0	100,0		
		1,1	0,0	0,4	7,1	5,8	35,8	8,0	0,7	2,0	0,0	8,7	0,0	0,2	25,1	2,9	0,7	0,0	0,7	0,9	0,0	100,0		
		16,7	0,0	0,6	19,2	23,2	0,4	1,3	6,9	0,0	0,0	1,5	0,0	23,4	4,6	0,0	1,5	0,0	0,4	0,2	0,0	100,0		
		15,7	0,0	0,0	13,8	10,5	1,5	5,0	14,0	0,5	0,3	4,8	0,0	0,0	14,0	9,5	10,3	0,0	0,0	0,3	0,0	100,0		
		22,4	0,7	0,2	18,7																			

from the in situ deposits. From a genetic perspective, the occurrence of neovolcanic nuclei underscores the strong link between syn-sedimentary volcanism and ooid formation in an alkaline lacustrine environment (Olazábal *et al.*, 2021). In these units, dawsonite (Fig. 4f) is particularly noteworthy and is associated with outcrops developed near a major fault at the northern end of Sierra Silva (Olazábal *et al.*, 2018).

The Castillo Formation

The Castillo Formation consists of fluvial channel-belt and floodplain deposits dominated by pale-grey reworked volcaniclastic strata with minor primary ash-fall deposits (Figs. 2a–c). This unit mainly represents multiple drainage catchments within a W–E elongated extensional basin, which was disconnected from the Cañadón Asfalto Basin (Paredes *et al.*, 2024). We attributed the elevated tuffaceous content within channel-belt deposits to the incorporation of unstable particles during high-energy floods following the deposition of ash-fall strata within the drainage catchments. In contrast, distal floodplain deposits were constructed by overbank processes during major flood events. These strata are interbedded with thin, primary pyroclastic layers containing accretionary lapilli, which indicate ash-fall events (Paredes *et al.*, 2021).

The earliest analyses of the Castillo Formation were conducted by Teruggi and Rossetto (1963) on exposures at the Codo del Río Senguerr. Their study identified a significant presence of andesitic-dacitic lithic fragments and clast of pyroclastic rocks of acidic origin. Petrographic studies along the SBFB (Tunik *et al.*, 2015) have documented variations in detrital composition linked to the hierarchy of formative drainage catchments, with smaller channel networks reflecting local sources and larger-scale channel networks showing regional-scale sediment provenance. In this regard, sandstones from La Angostura (Figs. 2b, 3c) were associated with poorly integrated drainage networks, containing a high proportion of paleovolcanic lithic fragments with lathwork and pilotaxitic textures, suggesting local sediment sources dominated by dense or sheet-like volcaniclastic flows that form small-scale channel-belt deposits (Tunik *et al.*, 2015). In contrast, sandstones from the Codo del Senguerr (Fig. 3c) were associated with well-integrated drainage networks that flowed toward ESE under more persistent hydrological conditions, likely following inherited, extensional structures (Paredes *et al.*, 2015). Detrital components

of medium-grained sandstones evidence a greater abundance of neovolcanic lithic fragments, in which acidic volcanic compositions predominate over basic and intermediate ones (Tunik *et al.*, 2015). These spatial compositional changes are associated with different drainage catchments coeval during the deposition of the Castillo Formation.

Expanding on these petrographic observations, the sandstone composition of the Castillo Formation shows significant variability across different localities. The ternary diagram (Fig. 3c) reveals that samples from La Angostura are grouped within the feldspatho-lithic field, with an average composition of Q7F35L58 (Table 1) indicating dominance of feldspar and pyroclastic lithic fragments (Fig. 4f) over quartz. Sedimentary and metamorphic lithic components are present within the lithic fraction, but subordinate (Olazábal *et al.*, 2020).

Beyond the compositional aspect, research on the Castillo Formation's diagenetic conditions has focused on dawsonite occurrence in the Sierra Silva anticline (Comerio *et al.*, 2014). Dawsonite occurs in tuffs and quartzo-lithic and litho-quartzose sandstones (Fig. 3c), which are dominated by volcanic and pyroclastic lithic clasts, with a low proportion of polycrystalline quartz and minor amounts of sedimentary and metamorphic lithics. On average, this mineral is associated with sandstones, where reworked pyroclastic fragments constitute nearly 25 % of the rock. Its formation is favored by the proximity of major faults and nearby Cenozoic intrusive bodies, likely sourced from hypabyssal, basic alkaline igneous rocks. In this particular location, the presence of dawsonite has also contributed to a reduction in the porosity of the host rock.

The arenites of the Castillo Formation are considered analogs of the Mina del Carmen reservoirs at the GSJB subsurface. Outcrop samples are characterized by a detrital composition dominated by volcanic and volcaniclastic lithic fragments with low quartz content (Fig. 3c). The high proportion of fine-grained volcaniclastic particles has reduced the reservoir quality of potential hydrocarbons in fluvial channel-belt deposits due to diagenetic alteration of volcanic glass (Tunik *et al.*, 2004). In contrast, subsurface samples from the SBFB (Fig. 3c) exhibit a predominantly feldspatho-lithic and litho-feldspathic compositions, with minor proportions of qLF, qFL, and lesser amount of IQF and fQL assemblages (Tunik *et al.*, 2006). The dominance of feldspar clast in the subsurface sandstones marks a significant compositional difference compared to outcrops along the SBFB.

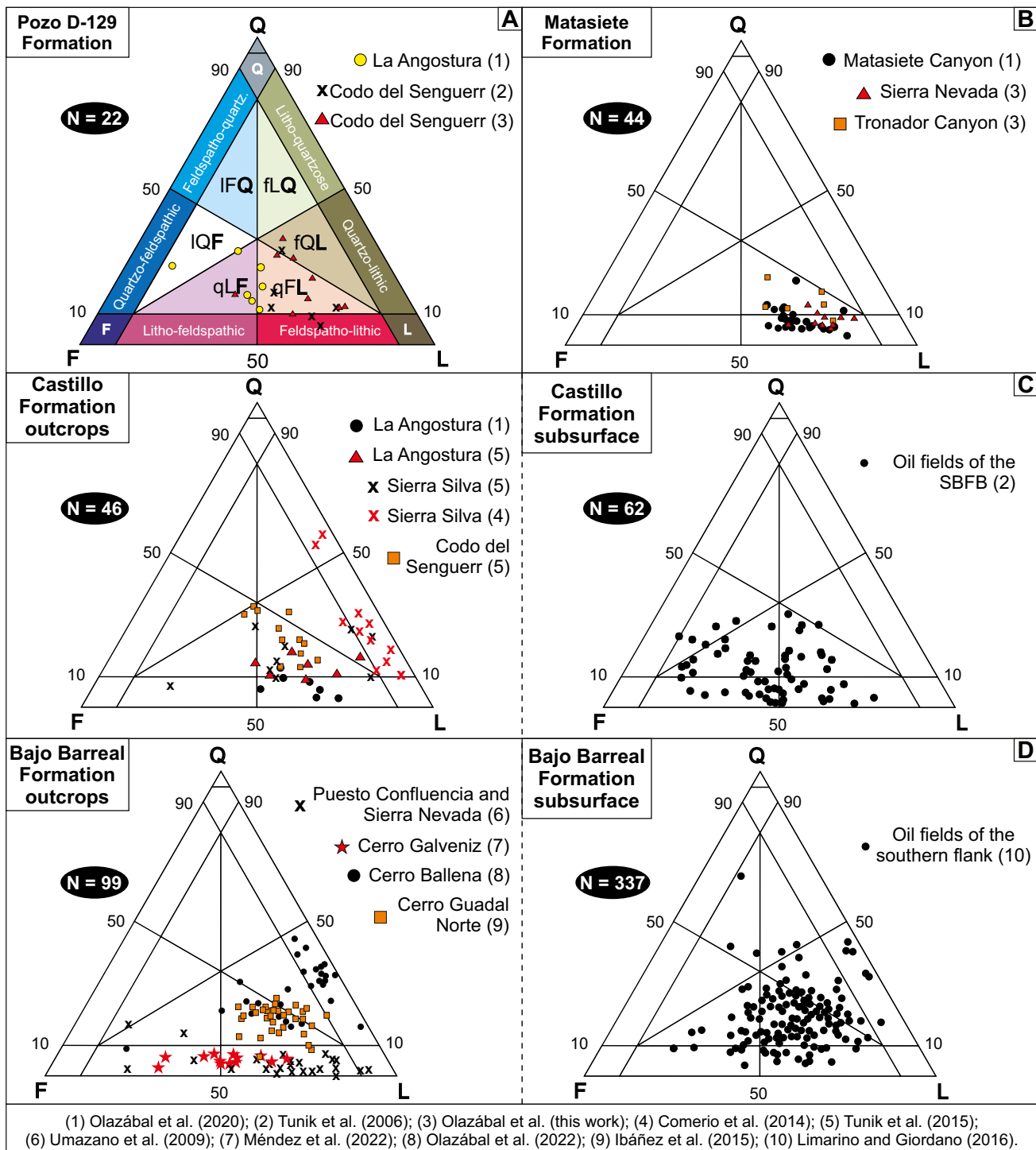


Figure 3. QFL ternary diagrams (Garzanti, 2019) depicting the sandstone composition of different stratigraphic units of the Chubut Group of the San Bernardo Fold Belt (SBFB). See Figure 1b for the location of the sampling sites. The total number of samples (N) is indicated for each dataset. The studies analyzed used the Gazzi-Dickinson point-counting method. **a)** Pozo D-129 Formation in La Angostura and Codo del Senguerr. **b)** Three members of Matasiete Formation in northern localities of the SBFB. **c)** Castillo Formation in outcrops (left) and subsurface (right). **d)** Bajo Barreal Formation in outcrops (left) and subsurface (right).

The Bajo Barreal Formation

Fluvial deposits of the Bajo Barreal Formation are widely distributed along the SBFB, and its detrital

modes show distinctive compositional differences across exposures. In the northernmost outcrops (Sierra Nevada and Puesto Confluencia), sandstones are predominantly feldspatho-lithic, with a lesser

proportion of litho-feldspathic, correlating to Qlf and L compositions (Umazano *et al.*, 2009) (Fig. 3d). These sandstones are characterized by an abundance of felsitic and acidic volcanic lithic fragments, with a low proportion of quartz. Southward, in the Cerro Colorado de Galveniz, sandstones exhibit feldspatho-lithic to litho-feldspathic compositions (Fig. 3d). However, these sandstones are distinguished by their remarkably clean clastic components and a distinctive green coloration, attributed to the presence of celadonite (Fig. 4h).

In contrast, Cerro Guadal Norte outcrops exhibit a different compositional trend, with sandstones primarily classified as qFL and a minor proportion of fQL and feldspatho-lithic compositions (Fig. 3d) (Ibáñez

et al., 2015). Their microfabrics show significant lateral and vertical variation in secondary porosity, ranging among 24 % and 18 %. The framework is enriched in volcanic and pyroclastic lithic fragments, reflecting a moderate influence from volcanic sources.

Further compositional variability is evident in Cerro Ballena anticline, where Olazábal *et al.* (2022) reported a dominance of quartzo-lithic, qFL, fQL, and litho-feldspathic (Fig. 3d). The framework is mainly composed of volcanic lithic fragments, acidic and felsitic lithic fragments (Fig. 4i), while metamorphic, sedimentary and polycrystalline quartz grains are subordinate. Although feldspars are in minor proportions, they commonly undergo dissolution or replacement by clays and carbonates during diagenesis.

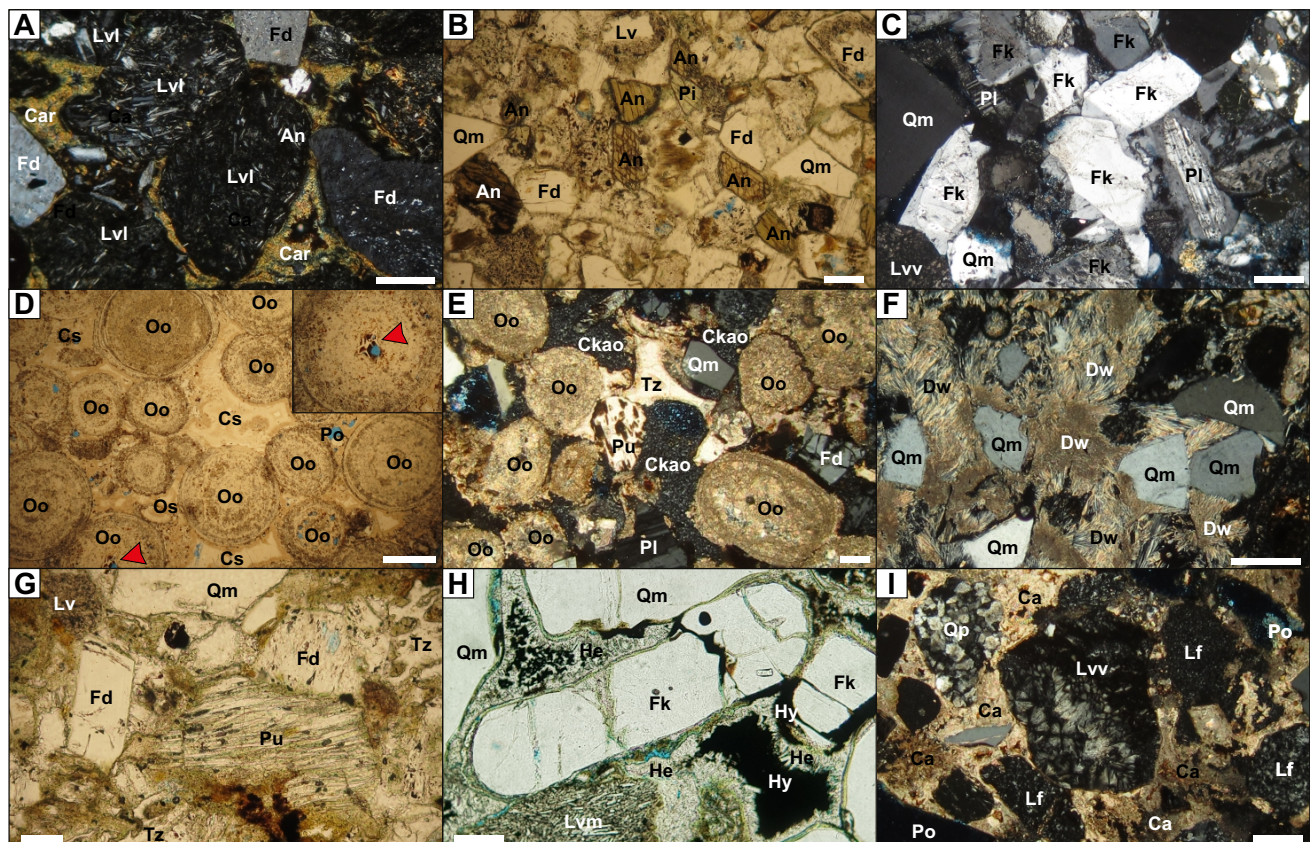


Figure 4. Microphotographs of sandstones from different formations under plane-polarized and cross-polarized light, highlighting key detrital and intergranular components. The graphical scale (white bar) represents 0.2 mm in all cases. **a)** Feldspatho-lithic sandstone of Matasiete Formation (Lower Member) in Cañadón Matasiete, with the presence of volcanic lithic grain with lathwork texture (Lvl), feldspars (Fd) and grain-coating of clay (Car). **b)** Feldspatho-lithic sandstone of Matasiete Formation (Upper Member) in Tronador Canyon, showing the presence of unstable heavy minerals such as amphiboles (An) and pyroxenes (Pi), volcanic lithic (Lv), monocrystalline quartz (Qm) and feldspars (Fd). **c)** IQF sandstone of Pozo D-129 Formation in La Angostura, with evidence of secondary overgrowth in alkaline feldspar (Fk), plagioclases (Pl) and monocrystalline quartz (Qm). **d)** Oolitic grainstone of Pozo D-129 Formation at Cerro Chenques, with ooids (Oo) containing vitric shard nuclei (red arrow) and significant silica cement (Cs). **e)** Mixed siliciclastic-carbonate-pyroclastic composition of Pozo D-129 Formation at Cerro Chenques, showing monocrystalline quartz (Qm), feldspars (Fd), and pumice lithic grain (Pu) and Y-shaped glass shards (Tz) entirely replaced by carbonate, with the presence of ooids (Oo). Note the intergranular pore filled with kaolinite cement (Ckao). **f)** Occurrence of Dawsonite (Dw) in sandstone of the Pozo D-129 Formation at Sierra Silva (Jerez Anticline). **g)** Feldspatho-lithic sandstone of the Castillo Formation in La Angostura featuring large, altered neovolcanic pumice lithic grain (Pu) and Y-shaped glass shards (Tz) associated with monocrystalline quartz (Qm) and feldspar (Fd). **h)** Litho-feldspathic sandstone of Bajo Barreal Formation in Cerro Colorado de Galveniz, with well-preserved feldspar (Fd), monocrystalline quartz (Qm), and volcanic lithic grains with microlithic texture (Lvm). Hydrocarbon impregnation (Hy) is observed, associated with heulandite-zeolitic and celadonite cementation and alteration. **i)** Quartzo-lithic sandstone of Bajo Barreal Formation in Cerro Ballena, characterized by volcanic lithic grain with vitric (Lvv) and felsitic (Lf) textures with intergranular pore filled of carbonate (Ca).

Unlike the compositional patterns observed in outcrops, subsurface samples from the South Flank exhibit a broader range of petrographic variability. Limarino and Giordano (2016) analyzed detrital modes from 337 sidewall cores and cutting samples (Fig. 3d), identifying a framework primarily dominated by volcanic clasts of variable composition and pyroclastic fragments. Notably, metamorphic, polycrystalline quartz, and sedimentary rock fragments also contribute to the assemblage, reaching up to 20 %. Dunn (1992) established two petrofacies of the Comodoro Rivadavia Formation (equivalent to the Bajo Barreal Formation) in areas located at the limits between the North Flank and the SBFB, with compositions Q27F21L52 and Q6F25L69, recognizing volcanic and basement-related lithologies that represent different drainage system attributable to varied provenance without further detail. Research on the distribution and origin of porosity in reservoir rocks of the South Flank has highlighted key diagenetic processes, particularly the dissolution of feldspar clasts and ductile fragments, which generate mesopores and macropores that significantly enhance permeability (Limarino *et al.*, 2020).

DISCUSSION

In this overview, a comprehensive petrographic analysis of the Pozo D-129, Matasiete, Castillo, and Bajo Barreal formations highlights the dynamic interplay between volcanic activity and sediment supply that shaped the sedimentary record of the Cretaceous Chubut Group in the Golfo San Jorge Basin. The evolution of sediment sources through time is closely linked to regional tectonic processes, active volcanism, and changes in sediment dispersal pathways.

Regional Source Areas and Sedimentary Routes

Vertical compositional trends in sandstones of the SBFB reveal variations in detrital modes, which reflect shifts in the lithology of the contributing source areas. Integrating detrital modes, paleoflow directions, and regional geology suggest potential source areas located to the NNE-NE of the studied localities (Olazábal *et al.*, 2020). These sources include the Paleozoic igneous-metamorphic basement—exposed in the Puesto La Potranca Formation and

the Catreleo granite—and Middle-Upper Jurassic volcanic and volcaniclastic rocks of the Lonco Trapial Group, exposed in the homonymous range and Cerro Negro (Olazábal *et al.*, 2020). Additionally, regional drainage networks could obtain similar lithics from intra-basin structural highs or the northern sector of the Cañadón Asfalto Basin. These source areas are well represented in the composition of fluvial channel sandstone deposits of the Matasiete Formation, which contain lithic fragments derived from mafic to intermediate volcanic sources, along with acidic and felsitic components. The observed southward reduction trend in heavy minerals such as pyroxenes and amphiboles between Tronador Canyon and Matasiete Canyon (~ 65 km) (Fig. 1b) is consistent with hydraulic sorting processes, differential mechanical and chemical durability of these unstable phases during transportation, leading to their progressive depletion along the transport pathway (Olazábal *et al.*, 2023).

A distinctive provenance signal emerges from the acidic and pyroclastic neovolcanic lithics recorded in the Pozo D-129, Castillo, and Bajo Barreal formations. These lithics are associated with input from the contemporaneous Andean arc through direct fallout and mainly reworking by fluvial systems (Tunik *et al.*, 2006; Umazano *et al.*, 2009; Tunik *et al.*, 2015; Olazábal *et al.*, 2020). The predominance of arc-derived detritus, with compositions ranging from felsic to intermediate, suggests a strong influence from Jurassic volcanic rocks and Cretaceous pyroclastic deposits. Furthermore, the geochemical affinity of these sandstones with Upper Cretaceous volcanic rocks assigned to the Divisadero Group supports their derivation from an active magmatic arc (Umazano *et al.*, 2009).

This signal indicates that reworked volcanic ash dominated fluvial headwaters, with transport and deposition conditioned by channel morphology and sediment transport capacity (Olazábal *et al.*, 2020). These compositional signals highlight the role of volcaniclastic material in shaping regional sedimentary systems.

In contrast to the compositional patterns observed in outcrops along the SBFB, subsurface samples from the South Flank exhibit a broader range of petrographic features. Limarino and Giordano (2016) identified six distinct petrofacies associated with different source areas, reflecting a primary contribution from Jurassic volcanic rocks, a

distal volcaniclastic source of Cretaceous age linked to coeval active volcanism along the Andes, and a subordinate input from basement-derived rock fragments.

Future perspectives

Despite these advancements, several important topics require further study. For example, the origin of the informal member “Areniscas Verdes” of the Bajo Barreal Formation. This petrographic signal remains unexplored, possibly linked to hydrocarbon bleaching (Zhang *et al.*, 2019), although this hypothesis requires further research to assess the role of structural diagenesis. On the other hand, the uppermost units within the Chubut Group, such as the Laguna Palacios and Lago Colhué Huapi formations, remain largely uncharacterized from a petrographic perspective. Conducting detailed studies on these units would contribute to a more comprehensive understanding of the compositional framework of the Chubut Group. Additionally, further research is required to assess how diagenetic processes modify detrital modes, as post-depositional alterations can significantly impact on primary compositions. In this context, evaluating the effects of structural diagenesis associated with tectonic inversion and telogenesis resulting from outcrop exhumation is crucial.

Integrating provenance studies with detrital geochronology remains a key challenge. This approach is particularly complex due to the high volcaniclastic input, which is closely linked to the residence time of tuffaceous material in headwater regions. Moreover, future research should incorporate thermochronological analyses to better constrain the evolution of source areas. Heavy mineral analysis is another promising but underexplored technique that could provide insights into specific source rock compositions.

From an applied perspective, it is essential to investigate the distribution and controlling factors of zeolitic and clay cement both in outcrops and the subsurface, as well as the origin of specific minerals such as dawsonite and celadonite. These aspects are particularly relevant for optimizing hydrocarbon production strategies and developing mitigation approaches for climate change, including CO₂ geological sequestration and the storage of Green and Blue hydrogen (Manzanal *et al.*, 2024; Tunik *et al.*, 2024).

CONCLUSIONS

Detrital modes and sedimentary petrography are fundamental tools for reconstructing sedimentary pathways and identifying source areas in fluvial systems. This study presents a comprehensive synthesis of the petrography of the Chubut Group, emphasizing its compositional variability and the primary controls on sediment supply.

Petrographic analysis of sandstones reveals a predominantly feldspatho-lithic to litho-feldspathic composition, ranging from qFL, fQL, and IQF to qLF assemblages, with compositional variations across units indicating shifts in provenance and fluctuations in sediment supply. The sedimentary petrography of the Chubut Group reflects a complex compositional evolution influenced by heterogeneous source rocks and variable volcaniclastic input.

The presence of lithic fragments of diverse compositions, along with multiple feldspar and quartz types, underscores the contribution of multiple source areas, including recycled Jurassic syn-rift and pre-rift substrates, as well as input from the crystalline basement. Across all units, a substantial and persistent sediment influx originated from active Andean arc volcanism to the west of the basin, either through direct volcanic ash fallout or the reworking of volcaniclastic material.

The regional paleogeographic framework and the distribution of pre-Chubut Group rocks constrain the definition of source areas. The Matasiete–Pozo D-129 depositional system provides the most extensive and well-constrained paleogeographic reconstruction, including spatially and temporally linked outcrops. In the northernmost sector of the SBFB, particularly within the Matasiete Formation, sediment supply was derived from mafic to intermediate lithologies of the Lonco Trapial Complex, as well as acidic and pyroclastic sequences of the Marifil Group. These exotic fluvial routes developed within extensional corridors controlled by inherited paleohighs, which regulated the highly variable composition of transverse sediment supply. In this broader context, downstream trends in heavy mineral components reflect localized inputs and hydraulic sorting processes.

The Castillo Formation is associated with a volcaniclastic maximum, where fluvial systems increase in paleodrainage efficiency southward. However, petrographic studies remain sparse and

disconnected mainly from specific sedimentary pathways. Despite these uncertainties, there is a clear trend of increasing feldspar content in subsurface petrofacies relative to outcrop samples. This trend may reflect the influence of regional tributary fluvial systems transporting sediments toward depocenters, which will dilute neovolcanic lithic components and a relative enrichment of crystalline basement-derived sediments. In contrast, northern localities with smaller, more localized headwater systems exhibit an enrichment in neovolcanic components.

The Bajo Barreal Formation presents a broader geographic distribution of sampled localities, facilitating the identification of peripheral source areas. In this context, sediment input from the Deseado Region and the crystalline basement characterize the South Flank, whereas the SBFB records contributions from source areas of variable composition located westward, beyond the West Flank. As in the previously discussed units, neovolcanic input from the contemporaneous Andean arc represents a consistent sedimentary signal across all studied regions.

Acknowledgements. The authors thanks to the Department of Geology (FCNyCS - UNPSJB) for logistical support. S.X. Olazábal gratefully acknowledges the funding from CONICET through the doctoral completion scholarship and expresses deep gratitude to the Argentine public education system.

REFERENCES

- Allard, J.O., Paredes, J.M., Foix, N., and Giacosa, R.E. (2015). Conexión cretácica entre las cuencas del Golfo San Jorge y Cañadón Asfalto (Patagonia): paleogeografía, implicancias tectonoestratigráficas y su potencial en la exploración de hidrocarburos. *Revista de la Asociación Geológica Argentina* 72(1), 21–37. <https://revista.geologica.org.ar/raga/article/view/372>.
- Allard, J.O., Foix, N., Urrez, N., and Cuello, M.J. (2022). *Edades U-Pb del Grupo Chubut en el Codo del Senguer, Cuenca del Golfo San Jorge (Patagonia extraandina): calibración cronoestratigráfica e impacto en el análisis del Sistema petrolero. Sesiones Generales XI Congreso de Exploración y Desarrollo de Hidrocarburos*, pp. 215–243.
- Allard, J.O., Foix, N., Paredes, J.M., Giacosa, R.E., Bueti, S., Oporto, F.E., and Rodríguez, A. (2025). Structural evolution of the Golfo San Jorge Basin: a comprehensive synthesis. *Latin American Journal of Sedimentology and Basin Analysis* 32(1), 19–31.
- Allen, P.A. (2017). *Sediment routing systems: the fate of sediment from source to sink*. Imperial College of Science, Technology and Medicine, pp. 407. London.
- Basile, Y.A., Utgé, S.M., Martínez Cal, V., and Ponce, C. (2014). *Avances en el conocimiento sobre la capacidad generadora de la Fm. Pozo D-129: aspectos litológicos y geoquímicos. Cuenca del Golfo San Jorge, Argentina. Trabajos Técnicos IX Congreso de Exploración y Desarrollo de Hidrocarburos*, pp. 264–285.
- Casal, G.A., Allard, J.O., and Foix, N. (2015). Análisis estratigráfico y paleontológico del Cretácico superior en la cuenca del Golfo San Jorge: nueva unidad litoestratigráfica para el Grupo Chubut. *Revista Asociación Geológica Argentina* 72, 81–99.
- Casal, G.A., Ibiricu, L.M., and Martínez, R.D. (2021). Vertebrados continentales cretácicos del Grupo Chubut. In: Giacosa, R.E. (Ed.), *Relatorio de Geología y Recursos Naturales de la Provincia de Chubut*, F2, pp. 806–833.
- Comerio, M., Morosi, M., Tunik, M., Paredes, J.M., and Zalba, P. (2014). The role of telogenetic injection of magmatically derived CO₂ in the formation of dawsonite from the Castillo Formation, Chubut Group, Patagonia, Argentina. *The Canadian Mineralogist* 52, 513–531. <https://doi.org/10.3749/canmin.52.3.513>.
- Dickinson, W.R. (1985). Interpreting provenance relations from detrital modes of sandstones. In: Zuffa, G.G. (Ed.), *Provenance of Arenites*. Reidel Publishing Company, pp. 333–361.
- Dickinson, W.R., Beard, L.S., Brakenridge, G.R., Erjavec, J.L., Ferguson, R.C., Inman, K.F., Kneppe, R.A., Lindberg, F.A., and Ryberg, P.T. (1983). Provenance of North American Phanerozoic sandstones in relation to tectonic setting. *Geological Society of America Bulletin* 94, 222–235.
- Dunn, T.L. (1992). Infiltrated Materials in Cretaceous Volcanogenic Sandstones, San Jorge Basin, Argentina. In: Houseknecht, D.W., Pittman, E.D. (Eds.), *Origin, Diagenesis and Petrophysics of Clay Minerals in Sandstones*. SEPM Special Publication 47, pp. 159–174. Tulsa, Ok.
- Figari, E.G., Scasso, R.A., Cúneo, R.N., and Escapa, I. (2015). Estratigrafía y evolución geológica de la cuenca de Cañadón Asfalto, Provincia del Chubut, Argentina. *Latin American Journal of Sedimentology and Basin Analysis* 22(2), 135–169.
- Figari E.G., Hechem, J.J., Continanza, M.J., Gavarrino, A., Urrez, N., and García D. (2021). Cuencas hidrocarburíferas, sus sistemas petroleras y principales yacimientos. In: Giacosa, R.E. (Ed.), *Relatorio de Geología y Recursos Naturales de la Provincia de Chubut*, F2, pp. 1416–1448, Puerto Madryn.
- Foix, N., Paredes, J.M., Oporto, F.E., and Allard, J.O. (2025). Cenozoic Stratigraphy of the Golfo San Jorge Basin, Argentina. *Latin American Journal of Sedimentology and Basin Analysis* 32(1), 68–80.
- Garzanti, E. (2019). Petrographic classification of sand and sandstone. *Earth-Science Reviews* 192, 545–563.
- Giacosa, R.E. (2020). Basement control, sedimentary basin inception and early evolution of the Mesozoic basins in the Patagonian foreland. *Journal of South American Earth Sciences* 97, 102407.
- Ibáñez, L.M., Ovejero, R., Georgieff, S.M., Ferreira, L., and Bossi, G.E. (2015). Petrografía y porosidad de areniscas portadoras de petróleo. Formación Bajo Barreal (Cretácico), Cuenca Golfo San Jorge, Argentina. *Acta Geológica Lilloana* 27, 29–51.
- Lesta, P., Ferello, R., and Chebli, G. (1980). Chubut extraandino. En: Turner, J.C. (Ed.), *2º Simposio de Geología Regional Argentina, Academia Nacional de Ciencias* 2, 1307–1387, Córdoba.
- Limarino, C.O., and Giordano, S.R. (2016). Unraveling multiple provenance areas using sandstone petrofacies and geochemistry: An example in the southern flank of the Golfo San Jorge Basin (Patagonia, Argentina). *Journal*

- of *South American Earth Sciences* 66, 208–231. <https://doi.org/10.1016/j.jsames.2016.01.006>.
- Limarino, C.O., Giordano, S.R., Rodríguez Albertani, R.J., Ciccioli, P.L., and Bodan, F. (2020). Patterns and origins of the porosity in the productive reservoirs of the upper part of the Chubut Group, southern flank of the Golfo San Jorge Basin, Patagonia Argentina. *Journal of South American Earth Sciences* 98, 102480. <https://doi.org/10.1016/j.jsames.2019.102480>.
- Manzanal, D., Laskowski, C.B., Cortes, M., Vidal, P., and Allard, J.O. (2024). Geomechanical evaluation of analogs of reservoirs for geological storage of CO₂. XVIII European Conference on soil mechanics and geotechnical engineering, pp. 3123–3128. DOI 10.1201/9781003431749-613
- Méndez, F.L., Allard, J.O., Olazábal, S.X., and Bueti, S.A. (2022). Análisis microtectónico de bandas de deformación en arenitas de la Formación Bajo Barreal, cuenca del Golfo San Jorge. Programa de Estudiantes 11º Congreso de Exploración y Desarrollo de Hidrocarburos, pp. 27–34.
- Olazábal, S.X., Tunik, M.A., Paredes, J.M., Allard, J.O., and Foix, N. (2018). Primer hallazgo de Dawsonita en la Formación Pozo D-129 en el extremo norte de Sierra Silva (Cuenca del Golfo San Jorge). Actas XVI Reunión Argentina de Sedimentología, p. 62.
- Olazábal, S.X., Tunik, M.A., and Paredes, J.M. (2020). Sandstone petrography and provenance of the Chubut Group (Cretaceous) in the Matasiete Canyon (Golfo San Jorge Basin, central Patagonia): implication for basin evolution and alluvial organization. *Journal of South American Earth Sciences* 98, 102463 <https://doi.org/10.1016/j.jsames.2019.102463>.
- Olazábal, S.X., Paredes, J.M., Tunik, M.A., Allard, J.O., and Foix, N. (2021). Morfotípos de ooides de la Formación Pozo D-129 (Cuenca del Golfo San Jorge): génesis sin-eruptiva e implicancias paleoambientales. Actas XVII Reunión Argentina de Sedimentología y VIII Congreso Latinoamericano de Sedimentología, p. 169.
- Olazábal, S.X., Paredes, J.M., Allard, J.O., Foix, N., Valle, M.N., and Tunik, M.A. (2022). Influencia del aporte volcanoclástico en arenitas de la Formación Bajo Barreal (Cerro Ballena, Santa Cruz). Actas XXI Congreso Geológico Argentino, pp. 1537–1538.
- Olazábal, S.X., Paredes, J.M., Tunik, M.A., Allard, J.O., and Foix, N. (2023). Importancia de minerales pesados en la procedencia de la Formación Matasiete (Cuenca del Golfo San Jorge, Patagonia). Actas XVIII Reunión Argentina de Sedimentología y XI Congreso Latinoamericano de Sedimentología, p. 256.
- Paredes, J.M., Allard, J.O., Foix, N., Álvarez, B.N., and Olazábal, S.X. (2014). Sedimentología y perfiles de rayos gamma de la Formación Pozo D-129 en la Sierra de San Bernardo, Chubut. Trabajos Técnicos 9º Congreso de Exploración y Desarrollo de Hidrocarburos, pp. 455–479.
- Paredes, J.M., Foix, N., Allard, J.O., Colombo, F., and Tunik, M.A. (2015). Alluvial architecture of reworked pyroclastic deposits in peri-volcanic basins: Castillo Formation (Albian) of the Golfo San Jorge Basin, Argentina. *Revista de la Asociación Geológica Argentina* 72, 42–62. <https://revista.geologica.org.ar/raga/article/view/373>.
- Paredes, J.M., Foix, N., and Allard, J.O. (2021). Estratigrafía cretácica de la cuenca del Golfo San Jorge. In: Giacosa, R.E. (Ed.,), *Relatorio de Geología y Recursos Naturales de la Provincia de Chubut*, pp. 142–186.
- Paredes, J.M., Allard, J.O., Olazábal, S.X., Foix, N., Valle, M.N., and Tunik, M.A. (2024). Drainage reorganization and alluvial architecture of endorheic basins: The Lower Cretaceous record of the Chubut Group in the Golfo San Jorge Basin (Patagonia, Argentina). *Journal of South American Earth Sciences* 144, 105031. <https://doi.org/10.1016/j.jsames.2024.105031>.
- Paredes, J.M., Foix, N., Allard, J.O., Lizzoli, S., Olazábal, S.X., and Tunik, M.A. (2025). Stratigraphy of the Chubut Group (Cretaceous, Golfo San Jorge Basin, Patagonia): impacts of alloogenetic controls on the alluvial macro-architecture. *Latin American Journal of Sedimentology and Basin Analysis* 32(1), 32–43.
- Sciutto, J.C. (1981). *Geología del Codo del Río Senguerr, Chubut, Argentina. Actas 8º Congreso Geológico Argentino*, pp. 203–219.
- Teruggi, M.E., and Rossetto, H. (1963). Petrografía del chubutiano del Codo del Senguerr. *Boletín de Informaciones Petroleras* 354, pp. 18–35.
- Tunik, M.A., Vietto, M.E., Sciutto, J.C., and Estrada, E. (2004). Procedencia de areniscas del Grupo Chubut en el área central de la Sierra de San Bernardo. Análisis preliminar. *Revista de la Asociación Geológica Argentina* 59(4), 601–606.
- Tunik, M.A., Fernández, M.I., and Vietto, M.E. (2006). *Petrografía y procedencia de la Formación Castillo*. Informe final (Inédito) realizado para la empresa REPSOL-YPF. Parte I: 826 pp; Parte II: 296 pp.
- Tunik, M.A., Paredes, J.M., Fernández, M.I., Foix, N., and Allard, J.O. (2015). Análisis petrográfico de areniscas de la Formación Castillo (Albiano) en la faja plegada de San Bernardo, Cuenca Golfo San Jorge, Argentina. *Revista de la Asociación Geológica Argentina* 72, 63–80. <https://revista.geologica.org.ar/raga/article/view/374>.
- Tunik, M.A., Olazábal, S.X., Paredes, J.M., Allard, J.O., and Foix, N. (2024). Dawsonita en la Cuenca del Golfo San Jorge: potencial en Argentina para el almacenamiento subterráneo de CO₂. XXII Congreso Geológico Argentino, Actas, pp. 758–759.
- Umazano, A.M., Bellosi, E.S., Visconti, G., Jalfin, G.A., and Melchor, R.N. (2009). Sedimentary record of a Late Cretaceous volcanic arc in central Patagonia: petrography, geochemistry and provenance of fluvial volcaniclastic deposits of the Bajo Barreal Formation, San Jorge Basin, Argentina. *Cretaceous Research* 30, 749–766. <https://doi.org/10.1016/j.cretres.2008.12.015>.
- Zhang, L., Liu, C., and Lei, K. (2019). Green altered sandstone related to hydrocarbon migration from the uranium deposits in the northern Ordos Basin, China. *Ore Geology Reviews* 109, 482–493.